INSTITUTO DE FÍSICA

preprint

IFUSP/P-170

FORMALISM AND APPLICATIONS OF ELECTROFISSION AND PHOTOFISSION FRAGMENT ANGULAR DISTRIBUTIONS

by

J.D.T.Arruda Neto, S.B.Herdade and I.C.Nascimento

Institute of Physics, University of São Paulo, SP
Brazil

UNIVERSIDADE DE SÃO PAULO
INSTITUTO DE FÍSICA
Caixa Postal - 20.516
Cidade Universitária
São Paulo - BRASIL

FORMALISM AND APPLICATIONS OF ELECTROFISSION AND PHOTOFISSION FRAGMENT ANGULAR DISTRIBUTIONS *

J.D.T.Arruda Neto, S.B.Herdade and I.C.Nascimento

Institute of Physics, University of São Paulo, São Paulo, Brazil.

A B S T R A C T

A formalism for the joint analysis of angular distributions of electro and photofission fragments is presented, utilizing the virtual photon spectrum technique in DWBA. This formalism is applied to the study of angular distributions for the electrofission of ^{238}U, measured near the fission barrier, to obtain information about the low-lying levels (J^{π}, K) of the transition nucleus. The $(2^+,0)$, $(1^-,0)$, and $(1^-,1)$ levels, previously detected in photofission experiments, were confirmed. Evidences of a significant contributions of $(1^+,1)$, $(2^+,1)$ and $(2^+,2)$ levels are also presented.

* Supported in part by Fundação de Amparo è Pesquisa do Estado de São Paulo, Conselho Nacional de Desenvolvimento Científico e Tecnológico, and Financiadora de Estudos e Projetos.

MAR/79

KEYWORD ABSTRACT

[NUCLEAR REACTION ^{238}U(e,e'f), E=5.5-9 MeV, with electrons; measured fission-fragment angular distributions; deduced fission low-lying levels. Natural target.]

1. INTRODUCTION

In the last two decades the study of photofission fragment angular distributions, mainly in even-even nuclei, has proved to be an useful tool for the investigation of properties of fission barriers and for obtaining information on the fission channel spectrum. The status of these photofission studies for the actinides is reviewed in references [1,2].

Photofission cross sections exhibit, in general, a strong dependence on energy near the fission barrier requiring, therefore, intense photon fluxes for their measurement in the energy range 5-9 MeV. Most of the experiments in this energy region have been carried out using bremsstrahlung produced in electron accelerators[3-6]. Monochromatic neutron-capture gamma rays have also been used for the measurement of fission fragment angular distributions[7].

Another possibility, for the study of near barrier photofission, is the direct utilization of electron beams. This approach has not been, as yet, extensively used. The method consists in irradiating thin targets directly with electrons and measuring the fission yield at several angles with respect to the direction of the incident beam, for a given energy. The interaction between the electrons and the nucleus takes place through the virtual photon spectrum.

There are advantages of using the electroexcitation process in relation to photoexcitation. From the experimental point of view, the handling and monitoring of electron beams are easier than photon beams. By other side, the virtual photon spectra are not equal for different multipolarities[8] and this can enhance some nuclear transitions in relation to others. In this respect, because E2 and M1 virtual photon spectra are more intense than E1, angular distributions of electrofission fragments

may be, under certain conditions, more sensitive to those multipolarities in comparison to photofission.

Angular distributions in electron-induced fission of ^{232}Th have been obtained by Rasch et al[9], in the energy range 8.7 - 30.0 MeV; the bumps observed in the anisotropy have been attributed to second and third chance fission. Some results for the ^{238}U electrofission fragment angular distribution, in energies near the fission barrier, have been presented in a previous paper[10].

In the present paper, we introduce a formalism for the analysis of electrofission angular distributions on the basis of the virtual photon theory, in order to obtain information on the fissioning nucleus. The simultaneous analysis of the fission induced by virtual (electrofission) and real photons (photofission) is also introduced. The potentialities of this analysis have been indicated in our preliminary work[11], and subsequently by Onley and Bhandari[12]. The formalism here presented is applied to the analysis of fragment angular distributions in the electron-induced fission of ^{238}U.

2. THE FISSION MODE

The fission channel spectrum shows a rotational band structure, with quantum numbers determined by the symmetry of the nuclear deformation at the saddle point. The intrinsic quantum numbers that label the different channels include vibrational and quasi-particle excitation modes. Although the excitation energy of the fissioning nucleus is of the order of 5 MeV, the largest part of this energy is "storaged" as potential energy of deformation; we say that the nucleus is "cold" when passing by the saddle point. The quantized potential energy surfaces will be, therefore, well spaced as in the low energy spectrum. Figure 1 (taken from reference 1, pg. 42) shows, schematically, some possible collective bands for a transition even-even nucleus with a stable quandrupole deformation.

The dynamics of a fissioning nucleus may be compared with the dynamics of a symmetrical top. Since it is expected that scission occurs by separation of the fission fragments along the symmetry axis, it is assumed that the angular distribution of the fission fragments is determined by the distribution probability of the directions of the symmetry axis of a symmetrical top that presents the same quantum numbers J, M, K of the fissioning nucleus (figure 2).

3. ANGULAR DISTRIBUTION FUNCTION

A finite rotation of a reference system (x', y', z') with respect to the laboratory system (x,y,z) is described by the spherical function $D^{J}_{MK}(\alpha,\beta,\gamma)$, where (α,β,γ) are the Euler angles that define (x',y',z') with respect to (x,y,z). If we fix the system (x',y',z') to the nucleus, their rotations will be also described by the wave function:

$$\Psi^{J}_{MK}(\alpha,\beta,\gamma) = \sqrt{\frac{2J+1}{8\pi^2}} \cdot D^{J}_{MK}(\alpha,\beta,\gamma) \qquad (1)$$

If the z' axis is a symmetry axis of the nucleus, the probability of finding it between Ω and $\Omega+d\Omega$ is given by:

$$d^3P = \left|\Psi^{J}_{MK}(\alpha,\beta,\gamma)\right|^2 d\Omega = \frac{2J+1}{8\pi^2}\left|D^{J}_{MK}(\alpha,\beta,\gamma)\right|^2 \cdot$$

$$\cdot \sin\beta\, d\beta\, d\alpha\, d\gamma = \frac{2J+1}{8\pi^2} \cdot \left| e^{iM\alpha} \cdot d^{J}_{MK}(\beta) \cdot e^{iK\gamma}\right|^2 \cdot$$

$$\cdot \sin\beta\, d\beta\, d\alpha\, d\gamma$$

$$d^3P = \frac{2J+1}{8\pi^2}\left| d^{J}_{MK}(\beta)\right|^2 \cdot \sin\beta\, d\beta\, d\alpha\, d\gamma \qquad (2)$$

where

$$d^{J}_{MK}(\beta) = \left\{(J+M)!\,(J-M)!\,(J+K)!\,(J-K)!\right\}^{1/2} \cdot$$

$$\cdot \sum_{X} \frac{(-1)^X \cdot \left[\sin(\beta/2)\right]^{K+M+2X}}{(J-K-X)!} \cdot \frac{\left[\cos(\beta/2)\right]^{2J-K+M-2X}}{(J+M-X)!\,(X+K-M)!\,X!} \qquad (3)$$

X = 0,1,2,3,...n, where n is the maximum value of X for which the factors that appear in the denominator are non-negative.

The probability for z' to orientate between β and $\beta+d\beta$ is:

$$dP(\beta) = \int_{\alpha}\int_{\gamma} d^3P(\alpha,\beta,\gamma) = \frac{2J+1}{8\pi^2}\left|d^J_{MK}(\beta)\right|^2 \cdot$$

$$\cdot \sin\beta\, d\beta \int_0^{2\pi} d\alpha \int_0^{2\pi} d\gamma$$

$$dP(\beta) = \frac{(2J+1)}{2}\left|d^J_{MK}(\beta)\right|^2 \cdot \sin\beta\, d\beta$$

If it is assumed that the fission fragments separate along the nucleus symmetry axis, the angular distribution function is defined as:

$$W^J_{MK}(\beta) = \frac{(2J+1)}{2} \cdot \left|d^J_{MK}(\beta)\right|^2 \qquad (4)$$

with the normalization

$$\int_0^{\pi} W^J_{MK}(\beta) \sin\beta\, d\beta = 1 .$$

4. ANGULAR DISTRIBUTION OF PHOTOFISSION FRAGMENTS

The quantum numbers J and M are conserved in all the process of fission, through the various forms that the nucleus assumes in its way to scission. If K is also a good quantum number for the nucleus in its passage from the transition state (saddle point) to the separated fragments configuration, then the directional dependence of the fragments is univocally

determined. If, at the saddle point, the nucleus has a large deformation, which still could be considered as axially symmetric, then K could be considered a good quantum number; this hypothesis is confirmed by the success of the angular distribution analysis[1]. Suposing the existence of a double barrier for fission, it is assumed that the K distribution is "freezed" at the second barrier for low energy fission.

In what follows, we will consider only the fission fragment angular distribution for even-even nuclei (ground state 0^+).

The diferential photofission cross-section for a particular channel (J^π, K) is defined as:

$$\frac{d\sigma_\gamma}{d\Omega}\left(J^\pi; K; E, \underline{\theta}\right) = \sum_M \frac{\Phi_\gamma\left(J^\pi; K, M; E\right)}{2\pi} \cdot W^J_{MK}(\theta) \qquad (5)$$

where: $\underline{E}$ is the photon energy; $\underline{\theta}$ is the angle between the fission fragment path and the $\underline{z}$ axis (incident particle beam direction - Figure 2), in the laboratory system; $\underline{\Phi_\gamma}$ are the expansion coefficients; and $W^J_{MK}(\theta)$ is defined by equation 4.

For a photon of multipolarity L, absorbed by an even-even nucleus, we have $J^\pi = L^\pi$. For non-polarized photons we have:

$$\Phi_\gamma\left(L^\pi, K, M; E\right) = \Phi_\gamma\left(L^\pi, K, -M; E\right) \qquad \text{and}$$

$$\sigma_\gamma\left(L^\pi, K; E\right) = \sum_M \Phi_\gamma\left(L^\pi, K, M; E\right) \qquad (6)$$

is the cross-section for the (L^{π},K) channel. In photofission, the transferred angular momentum is limited to the magnetic sub-states with M=±1 (photon helicity). Then, from equation (6), it follows that: $\sigma_\gamma(L^\pi,K;E) = 2\,\phi_\gamma(L^\pi,K,1;E)$.

The total photofission cross-section, for all the multipole transitions involved, is given by:

$$\sigma_\gamma(E) = \sum_{L^\pi}\sum_{K}\sigma_\gamma(L^\pi,K;E) \quad ,$$

$$L^\pi = 1^-, 2^+, 1^+, 2^-, \ldots \text{ , and } K = 0, \pm1, \pm2, \ldots, \pm L \qquad (7)$$

The "total" angular distribution will be then:

$$\frac{d\sigma_\gamma}{d\Omega}(E,\theta) = \sum_{L^\pi}\sum_{K}\frac{d\sigma_\gamma}{d\Omega}(L^\pi,K;E,\theta) \qquad (8)$$

For E1, E2 and M1 transitions, L =1^-,2^+ and 1^+, respectively. Substituting (5) into (8):

$$\frac{d\sigma_\gamma}{d\Omega}(E,\theta) = \sum_{L^\pi=1^-,2^+,1^+}\sum_{K=0}^{\pm L}\frac{\phi_\gamma(L^\pi,K,M;E)}{2\pi}\cdot W^{L}_{MK}(\theta) \qquad (9)$$

Writing explicitly all the summations of (9), grouping, and using the simplified notation $\sigma_\gamma(L^\pi,K) = 2\phi_\gamma(L^\pi,K)$ we obtain:

$$\frac{d\sigma_\gamma}{d\Omega}(E,\theta) = \left[\frac{1}{4\pi}\left(3\sigma_\gamma(1^-,1) + 3\,\sigma_\gamma(1^+,1) + 5\,\sigma_\gamma(2^+,1)\right)\right] +$$

$$+ \left[\frac{1}{8\pi}\left(3\sigma_\gamma(1^-,0) - 3\sigma_\gamma(1^-,1) - 3\sigma_\gamma(1^+,1) + 5\sigma_\gamma(2^+,2) -\right.\right.$$

$$\left.\left. - 5\sigma_\gamma(2^+,1)\right)\right]\sin^2\theta + \left[\frac{5}{8\pi}\left(\frac{3}{4}\sigma_\gamma(2^+,0) - \sigma_\gamma(2^+,1) +\right.\right.$$

$$\left.\left. + \frac{1}{4}\sigma_\gamma(2^+,2)\right)\right]\sin^2(2\theta) =$$

$$= A_\gamma(E) + B_\gamma(E)\sin^2\theta + C_\gamma(E)\sin^2(2\theta) \qquad (10)$$

The coefficients A_γ, B_γ, and C_γ may be obtained by a least square fit of the expression (10) to the experimentally determined angular distributions. In general, these coefficients are presented in a normalized form with relation to the total photofission cross-section, that is, divided by:

$$\sigma_\gamma(E) = \int \frac{d\sigma_\gamma(E,\theta)}{d\Omega}\,d\Omega = 2\pi\left[2A_\gamma(E) + \right.$$

$$\left. + \frac{4}{3}B_\gamma(E) + \frac{16}{15}C_\gamma(E)\right] \qquad (11)$$

5. ANGULAR DISTRIBUTION OF ELECTROFISSION FRAGMENTS

In analogy to photofission (equation 5) we define, for electrofission:

$$\frac{d\sigma_e}{d\Omega}\left(L^{\pi},K;E_0,\theta\right)=\sum_{M=0}^{\pm L}\frac{\phi_e\left(L^{\pi},K,M;E_0\right)}{2\pi}\,W_{MK}^{L}(\theta) \qquad (12)$$

where E_o is the incident electron energy. As the virtual photon does not constitute a transverse plane wave, there will not be any restriction to the magnetic sub-states of the transferred angular momentum; therefore, M=0, ±1, ±2, ... ,±L.

The electrofission angular distribution is also a function of the transferred energy; then, each component of the distribution, ϕ_e, must be calculated by integration of the photofission cross-section multiplied by the virtual photon spectrum.

The total electrofission cross-section, for all the involved transitions, is given by:

$$\sigma_e\left(E_0\right)=\sum_{L^{\pi}}\sum_{K=0}^{\pm L}\sum_{M=0}^{\pm L}\phi_e\left(L^{\pi},K,M;E_0\right) \qquad (13)$$

The coefficients of the angular distributions, ϕ_e, are related to the photofission cross-section by means of the virtual photon formalism:

$$\phi_e\left(L^{\pi},K,M;E_0\right)=\int_0^{E_0}\sigma_\gamma\left(L^{\pi},K;E\right)N^{(\lambda L,M)}\left(E,E_0\right)\frac{dE}{E} \qquad (14)$$

where $N^{(\lambda L,M)}(E,E_0)$ is the virtual photon spectrum for a transition, with magnetic sub-state M, calculated in DWBA[8].

In analogy to photofission, considering E1, E2, and M1 transitions, we obtain:

$$\frac{d\sigma_e}{d\Omega}(E_0,\theta) = \sum_{L^\pi = 1^-,\,2^+,\,1^+} \sum_{K=0}^{\pm L} \frac{d\sigma_e}{d\Omega}(L^\pi, K; E_0, \theta) =$$

$$= A_e(E_0) + B_e(E_0)\sin^2\theta + C_e(E_0)\sin^2(2\theta)$$

where :

$$A_e = \frac{1}{4\pi}\Big[3\phi_e(1^-,0,0) + 3\phi_e(1^-,1,1) + 5\phi_e(2^+,0,0) +$$

$$+ 5\phi_e(2^+,1,1) + 5\phi_e(2^+,2,2) + 3\phi_e(1^+,1,1)\Big] \quad (15)$$

$$B_e = \frac{1}{4\pi}\Big[-3\phi_e(1^-,0,0) + \frac{3}{2}\phi_e(1^-,0,1) + 3\phi_e(1^-,1,0) -$$

$$- \frac{3}{2}\phi_e(1^-,1,1) - \frac{15}{4}\phi_e(2^+,0,0) + \frac{15}{8}\phi_e(2^+,0,2) -$$

$$- \frac{5}{2}\phi_e(2^+,1,1) + \frac{5}{2}\phi_e(2^+,1,2) + \frac{5}{4}\phi_e(2^+,2,0) + \frac{5}{2}\phi_e(2^+,2,1) -$$

$$- \frac{35}{8}\phi_e(2^+,2,2) + 3\phi_e(1^+,1,0) - \frac{3}{2}\phi_e(1^+,1,1)\Big] \quad (16)$$

$$C_e = \frac{15}{8\pi}\left[-\frac{9}{8}\phi_e(2^+;0,0) + \frac{3}{4}\phi_e(2^+;0,1) - \frac{3}{16}\phi_e(2^+;0,2) + \right.$$

$$+\frac{3}{2}\phi_e(2^+;1,0) - \phi_e(2^+;1,1) + \frac{1}{4}\phi_e(2^+;1,2) -$$

$$\left.-\frac{3}{8}\phi_e(2^+;2,0) + \frac{1}{4}\phi_e(2^+;2,1) - \frac{1}{16}\phi_e(2^+;2,2)\right] \quad (17)$$

6. COMBINED ANALYSIS OF ELECTRO- AND PHOTOFISSION ANGULAR DISTRIBUTIONS

Initially, it is interesting to find a relation between the angular distributions $d\sigma_\gamma/d\Omega$ and $d\sigma_e/d\Omega$, for photo- and electrofission, respectively. Substituting (14) in (12), we have:

$$\frac{d\sigma_e}{d\Omega}(L^\pi,K;E_0,\theta) = \sum_{M=0}^{\pm L}\frac{1}{2\pi}\int_0^{E_0}\sigma_\gamma(L^\pi,K;E)\,N^{(\lambda L,M)}(E,E_0).$$

$$W^L_{MK}(\theta)\frac{dE}{E} = \int_0^{E_0}\sum_{M=\pm 1}\frac{\sigma_\gamma(L^\pi,K;E)}{2\pi}W^L_{MK}(\theta)\cdot N^{(\lambda L,M)}(E,E_0)\frac{dE}{E} +$$

$$+\int_0^{E_0}\sum_{\substack{M=0\\ \neq\pm 1}}^{\pm L}\frac{\sigma_\gamma(L^\pi,K;E)}{2\pi}W^L_{MK}(\theta)\cdot N^{(\lambda L,M)}(E,E_0)\frac{dE}{E};$$

therefore:

$$\frac{d\sigma_e}{d\Omega}(L^\pi, K; E_0, \theta) = \int_0^{E_0} \frac{d\sigma_\gamma}{d\Omega}(L^\pi, K; E, \theta)\, N^{(\lambda L, 1)}(E, E_0)\, \frac{dE}{E} +$$

$$+ \int_0^{E_0} \frac{\sigma_\gamma(L^\pi, K; E)}{2\pi} \sum_{\substack{M=0 \\ \neq \pm 1}} W^L_{MK}(\theta)\, N^{(\lambda L, M)}(E, E_0)\, \frac{dE}{E} \qquad (18)$$

where $N^{(\lambda L, 1)} = N^{(\lambda L, +1)} + N^{(\lambda L, -1)}$

The result shown in equation 18 is important in the sense that it establishes clearly that, from a given photofission angular distribution $d\sigma_\gamma/d\Omega$ it is impossible to construct the corresponding electrofission angular distribution $d\sigma_e/d\Omega$ by means of the virtual photon formalism, unless the partial cross-sections $\sigma_\gamma(L^\pi, K; E)$ are known for all involved channels, which it is not the case.

A complete study of the fissioning nucleus, near the fission barrier, in a very general way, would involve the determination of six cross-sections related to the channels $(1^-,0)$, $(1^-,1)$, $(2^+,0)$, $(2^+,1)$, $(2^+,2)$, and $(1^+,1)$. This is possible, in principle, from the six coefficients: A_γ, B_γ, C_γ, A_e, B_e, C_e, although it is not trivial due to the complexity of the electrofission coefficients. Otherwise, only the coefficients C_γ and C_e are directly related to each other, allowing an analysis of the E2 fission channels, as will be shown in what follows.

Rewriting explicitly the functions ϕ_e (equation 17), in terms of the integrals given by equation 14, and grouping all the terms, we obtain:

$$C_\ell(E_0) = \frac{5}{128\pi} \int_0^{E_0} \left[3\sigma_\gamma(2^+,0) - 4\sigma_\gamma(2^+,1) + \sigma_\gamma(2^+,2) \right] \cdot$$

$$\cdot \left[-6\, N^{(E2,0)}(E,E_0) + 4\, N^{(E2,1)}(E,E_0) - N^{(E2,2)}(E,E_0) \right] \frac{dE}{E} \qquad (19)$$

Remembering that $C_\gamma = \frac{5}{32\pi}\left(3\sigma_\gamma(2^+,0) - 4\sigma_\gamma(2^+,1) + \sigma_\gamma(2^+,2)\right)$, and substituting in (19):

$$C_\ell(E_0) = \int_0^{E_0} C_\gamma(E)\; N^{(E2,*)}(E,E_0)\, \frac{dE}{E} \qquad (20)$$

where

$$N^{(E2,*)}(E,E_0) = \frac{1}{4}\left[-6\, N^{(E2,0)}(E,E_0) + 4\, N^{(E2,1)}(E,E_0) - N^{(E2,2)}(E,E_0) \right] \qquad (21)$$

Figures 3^a and 3^b show, as an example, the virtual photon spectra for Z=92 and E_o=9,5 MeV, corresponding to E1 and E2, respectively.

7. POTENTIALITIES AND APPLICATIONS OF THE FORMALISM

7.1 ^{238}U PHOTOFISSION DATA FROM THE LITERATURE

The angular distributions of photofission fragments, analysed near the fission barrier, have given information about the fission channel spectra, mainly for the $(1^-,0)$, $(1^-,1)$ and $(2^+,0)$ levels. There are no conclusive informations about the $(2^+,1)$ and $(2^+,2)$ levels, or still on a probable $(1^+,1)$ level. The main reason for this lack of information is that the C_γ coefficient, that represents the E2 contributions, is too small relatively to the A_γ and B_γ coefficients, the uncertainties involved in its experimental determination being very large at about 1 to 2 MeV above the fission barrier. Up to the present, only the $(1^-,0)$ channel has been undoubtedly identified for ^{238}U, by means of a proheminent structure in the photofission cross-section at 6.2 MeV, by several authors [4,7,13]. Table I shows some results for ^{238}U. Anderl et al.[13] detected also a pronounced structure at 7.6 MeV where intrinsic excitations dominate.

In electrofission, as will be shown in sections 7.2 and 7.3, the possibilities for the angular distribution analysis are greater in comparison with photofission, mainly with respect to the E2 component, because the C_e coefficient, equation 20, is significant as compared with the B_e and A_e coefficients, a few MeV's abcve the barrier. The higher intensity of the E2 virtual photon spectra, relatively to E1, enhances the E2 component of the electrofission angular distribution.

7.2 COMBINED ANALYSIS OF ELECTROFISSION AND PHOTOFISSION OF ^{238}U

For the utilization of the formalism presented in this paper, the ^{238}U electrofission fragment angular distribution was

measured from 5.5 to 9.0 MeV, by utilizing the electron beam of the University of São Paulo Linear Accelerator. The fission fragments were detected by mica foils placed in angles from 10^{o} to 120^{o} with respect to the incident electron beam. The experimental apparatus has been described in detail in a previous paper[14]. Figures 6 and 7 present some of the results that will be discussed.

Recently, Arruda Neto et al.[10,15] have developed a new method that enables the obtention of the total cross-section for multipoles different than E1, σ_{γ}^{Add}, involved in photonuclear reactions. This method consists in a combined analysis of the cross-sections for electro- and photoexcitations via the virtual photon formalism in DWBA. Figure 4[10] shows the cross section $\sigma_{\gamma,f}^{Add}(E)$, obtained by means of the above mentioned method, for the photofission of ^{238}U, that corresponds to the E2 and M1 contributions; the M1 contribution is included in $\sigma_{\gamma,f}^{Add}(E)$ amplified by an average factor $\left\langle \frac{N^{(M1)}}{N^{(E2)}} \right\rangle \simeq 3$, in the energy region 6 to 7 MeV. A tentative separation of E2 and M1 resulted in the cross-sections shown in Figure 5[10]. Similar results were recently obtained for the photofission of ^{236}U[16].

The C_e coefficients in the electrofission fragment angular distributions, obtained experimentally in the present study, may be utilized as a test for the reliability of the separation of the contributions of E2 and M1 in $\sigma_{\gamma,f}^{Add}(E)$ as will be discussed next.

Suposing initially that: $\sigma_{\gamma,f}^{(E2)} \simeq \sigma_{\gamma,f}^{(2^+,0)}$ near the fission barrier, from equation 20 we have:

$$C_e(E_0) = \frac{15}{32\pi} \int_0^{E_0} \sigma_{\gamma,f}^{(2^+,0)}(E)\, N^{(E2,*)}(E,E_0)\, \frac{dE}{E} \qquad (22)$$

T A B L E I

Low-lying levels in the ^{238}U transition nucleus, identified in photofission.

(L^{π},K)	Energy(13) MeV	Threshold (MeV)	
		REF.4	REF.7
$(2^{+},0)$	5.5	5.0	4.5 ± 3.3
$(1^{-},0)$	6.2	5.7	5.98 ± 0.06
$(1^{-},1)$	6.6 to 7.0	7.0	6.63 ± 0.04

The result of the numerical integration, using $\sigma_{\gamma f}^{E2}$ from reference 10, is presented by the solid line of Figure 6, together with the experimental values obtained for $C_e(E_o)$, that will be refered to as $C_e^{exp}(E_o)$. It is observed that, for electrons of energy $E_o \gtrsim 7$ MeV, C_e deviates systematically from C_e^{exp}, while below 7 MeV the agreement is reasonable. The dashed curve of Figure 6 represents the result of the calculation of the integral of equation 22 suposing that $\sigma_{\gamma f}^{(2^+,0)} = \sigma_{\gamma f}^{Add}$, that is, suposing that the M1 contribution is negligible and so $\sigma_{\gamma f}^{Add} \simeq \sigma_{\gamma f}^{E2}$; the disagreement is clearly shown. These facts suggest some important conclusions, as follows:

a) There is a non-negligible M1 contribution to the photofission of ^{238}U between 6 and 7 MeV;

b) The M1 strength, present in ^{238}U, must be of the order of magnitude of that estimated in reference 10 and shown in Figure 5;

c) A $(2^+,1)$ channel is opened at about E_o=7MeV, or its effect becomes appreciable above this energy, in the electrofission of ^{238}U; it is observed that (equation 19) the opening of a $(2^+,1)$ channel actuates in the sense to decrease C_e while the opening of an $(2^+,2)$ channel actuates in the sense to increase C_e.

This same analysis was made for ^{236}U, with similar results[16].

7.3 ELECTROFISSION CHANNEL ANALYSIS

As was commented in section 7.1, Figure 7 shows clearly the higher sensibility of electrofission, when compared to photofission, to detect E2 and M1 components. It can be verified also that the structures in C_γ/B_γ, between 7 and 8 MeV, are slightly suggested by the results obtained with bremsstrahlung, due to

the low resolution of this technique, while the data obtained with monochromatic neutron capture gamma rays accentuate a little more the structures, although with large experimental uncertainties. In electrofission it is easier to obtain results with better statistics, besides the fact that $C_e \approx B_e$, making possible the observation of finer details in the behaviour of C_e/B_e as a function of incident electron energy.

For an analysis of the reaction channels involved in photofission, by means of C_e and B_e, we must write these quantities explicitly as functions of the photofission cross-sections corresponding to the several channels. For C_e we have already written equation 20. For B_e, from equations 14 and 16, we have:

$$B_e(E_0) = \frac{1}{4\pi}\left\{\int_0^{E_0}\left[\sigma_\gamma(1^-,0) - \sigma_\gamma(1^-,1)\right] N^{(E1,*)}(E,E_0)\frac{dE}{E} - \right.$$

$$- \int_0^{E_0} \sigma_\gamma(1^+,1)\, N^{(M1,*)}(E,E_0)\frac{dE}{E} - \int_0^{E_0} \sigma_\gamma(2^+,1)\, N^{(E2,\Delta)}(E,E_0)\frac{dE}{E} -$$

$$\left. - \int_0^{E_0} \sigma_\gamma(2^+,0)\left[\frac{15}{4} N^{(E2,0)}(E,E_0) - \frac{15}{8} N^{(E2,2)}(E,E_0)\right]\frac{dE}{E}\right\} \quad (23)$$

where:

$$N^{(E1,*)} = \frac{3}{2} N^{(E1,1)} - 3 N^{(E1,0)}$$

$$N^{(M1,*)} = \frac{3}{2} N^{(M1,1)} - 3 N^{(M1,0)}$$

$$N^{(E2,\Delta)} = \frac{5}{2}\left[N^{(E2,1)} - N^{(E2,2)} \right]$$

Some comments on equation 23: the last term, in $\sigma_\gamma(2^+,0)$, is negligible because $\frac{15}{4} N^{(E2,0)} - \frac{15}{8} N^{(E2,2)} \simeq 0$ (see figure 3), in comparison with the virtual photon spectra in the remaining terms; the term in $\sigma_\gamma(2^+,1)$ is also negligible below 7 MeV (see comments in the end of section 7.2).

By inspection of C_e/B_e vs E_o, Figure 7, we observe that:

a) the ratio C_e/B_e (and also C_γ/B_γ) presents a relatively high value at about 5.5 MeV, that corresponds to the $(2^+,0)$ channel;

b) it decreases until about 6.5 MeV due to the opening of the $(1^-,0)$ channel (check with Table I);

c) it increases again until about 7.1 MeV due to the presence of the channels $(1^-,1)$ and $(1^+,1)$ that actuate in the sense of decreasing B_e (see equation 23).

Until this point the information obtained from C_e/B_e confirms the results obtained from photofission (Table I) which, on the other side, do not present enough sensibility to conclude anything about other E2 channels, $(2^+,1)$ and $(2^+,2)$. Continuing the analysis of Figure 7, we have:

d) C_e/B_e decreases again for $7.0 \lesssim E_o \lesssim 7.4$ MeV, probably due to the opening of the $(2^+,1)$ channel, confirming the limit imposed to this channel by the comparison of the E2 cross-section[10] with the C_e coefficient (section 7.2 and Figure 6).

e) C_e/B_e increases again for $7.4 \lesssim E_o \lesssim 7.8$ MeV; at this point of the analysis, with 5 channels opened it becomes difficult to interpret the oscilations of the experimental points in terms of the influence of a single channel or even to predict the opening of new channels; although, it is not totally excluded the possibility that this behaviour of C_e/B_e, in this energy region, is due to the opening of the $(2^+,2)$ channel.

8. CONCLUSIONS

The analysis of electrofission fragment angular distributions, with the formalism here presented, open new perspectives in the study of low-lying levels of fissioning (transition) nuclei. In the present paper, besides the confirmation of the results obtained from photofission relatively to the channels $(1^-,0)$, $(1^-,1)$ and $(2^+,0)$, it is established, for the first time, the competition of the channels $(2^+,0)$ and $(2^+,1)$ in the photofission of ^{238}U (Figure 6). Other important result is the confirmation of the presence of a dectetable M1 component, between 6 and 7 MeV in the photofission of ^{238}U. Also, the cross-section shown in Figure 5 is characterized as being due to the $(2^+,0)$ channel, up to $E_o \tilde{=} 7$ MeV.

The present analysis may be also used at lower energies ($E_o < 5.5$MeV) in order to study the sub-barrier anomalies in the photofission of heavy nuclei observed, up to the present, in experiments using bremsstrahlung [17,18]. As was discussed, electrofission fragment angular distributions are much more sensitive than photofission to the contributions of the several fission channels, what could be useful for the study of sub-barrier fission.

ACKNOWLEDGMENTS

The authors wish to thank Professor D.S. Onley and Dr. B.S. Bhandari for valuable discussions. We are also indebted to A. Vannucci and R. Hermann for their assistance in data handling.

REFERENCES

1) R.Vandenbosch and J.R.Huizenga; "Nuclear Fission", (Academic Press, N.Y., 1973) cap. V.

2) B.S.Bhandari and I.C.Nascimento; Nucl.Sci. & Eng. 60 (1976)19.

3) A.S.Soldatov, G.N.Smirenkin, S.P.Kapitza and Yu.M.Tsipenyuk; Phys.Lett. 14 (1965) 217.

4) N.S.Rabotnov, G.N.Smirenkin, A.S.Soldatov, L.N.Usachev, S.P. Kapitza and Yu.M. Tsipenyuk; Sov.J.Nucl.Phys.11 (1970)285.

5) A.V.Ignatyuk, N.S.Rabotnov, G.N.Smirenkin, A.S.Soldatov and Yu.M.Tsipenyuk; Sov.Phys. JETP 34 (1972) 684.

6) L.J.Lindgren, A.Alm and A.Sandell; Nucl.Phys. A298 (1978) 43.

7) E.J.Dowdy and T.L.Krysinski; Nucl.Phys. A175 (1971) 501.

8) W.W.Gargaro and D.S.Onley; Phys.Rev.C4 (1971) 1032.

9) P.Rasch, G.Fiedler and E.Konecny; Nucl.Phys. A219 (1974) 397.

10) J.D.T.Arruda Neto, S.B.Herdade, B.S.Bhandari and I.C.Nascimento; Phys.Rev. C18 (1978) 863.

11) J.D.T.Arruda Neto, B.S.Bhandari, S.B.Herdade and I.C.Nascimento; Ciência e Cultura 28, nº7 Supl. (1976) 53; abstract in Portuguese.

12) D.S.Onley and B.S.Bhandari; preprint IFUSP/P-94 (1976).

13) R.A.Anderl, M.V.Yester and R.C.Morrison; Nucl.Phys. A212 (1973) 221.

14) J.D.T.Arruda Neto, S.B.Herdade, B.S.Bhandari and I.C.Nascimento; Phys.Rev. C14 (1976) 1499.

15) J.D.T.Arruda Neto, "Giant Quadrupole Resonances in the Photofission of ^{236}U and ^{238}U", PhD Thesis, University of São Paulo (in Portuguese) (1977).

16) J.D.T. Arruda Neto, B.L.Berman, S.B.Herdade and I.C.Nascimento; "Measurements of the Giant E2 and M1 Resonances for ^{236}U", Preprint IFUSP/P-154, submitted to Physics Letters (1978).

17) C.D.Bowman, I.G.Schröder, C.E.Dick and M.E.Jackson; Phys.Rev. C12 (1975) 863.

18) V.E.Zhuko, A.V.Ignatyuk, A.S.Soldatov and Yu.M.Tsipenyuk; Phys.Lett. 68B (1977). 323.

FIGURE CAPTIONS

FIG. 1 - Schematic diagram of some possible collective band structures for an even-even transition nucleus with a stable quadrupole deformation[1].

FIG. 2 - Angular momentum coupling scheme for a deformed nucleus. R represents the collective rotational angular momentum; the other symbols are defined in the text.

FIG.3a - E1 virtual photon spectrum calculated in DWBA[8] for a Z=92 nucleus, showing the contributions of magnetic substates.

FIG.3b - The same as 3a for E2 virtual photons.

FIG. 4 - The cross section $\sigma_{\gamma,f}^{Add}$, as a function of the photon energy, which represents the contributions of multipoles transitions other than E1 in the photofission of ^{238}U[10].

FIG. 5 - The E2 and M1 components of $\sigma_{\gamma,f}^{Add}$, as a function of the photon energy[10].

FIG. 6 - The circles with error bars represent C_e^{exp} (see text), obtained by least square fits of the function $W(\theta) = A_e + B_e \sin^2\theta + C_e \sin^2(2\theta)$ to the experimental ^{238}U electrofission fragment angular distributions. The dashed curve is the result of the integral $\frac{15}{32\pi}\int_0^{E_0}\sigma_{\gamma,f}(2^+,0)\,N^{(E2,*)}(E,E_0)\frac{dE}{E}$, eq.22, where $\sigma_{\gamma,f}(2^+,0)=\sigma_{\gamma,f}^{Add}$. The continuous curve represents the same integral with $\sigma_{\gamma,f}(2^+,0)=\sigma_{\gamma,f}^{(E2)}$.

FIG. 7 - The points ⊙ and the continuous curve represent the ratios C_γ/B_γ of ^{238}U photofission fragment angular distributions as a function of the photon energy, taken from Dowdy and Krysinski[7] and Rabotnov et al.[4], respectively. The points ⊡ represent the ratios C_e/B_e of ^{238}U electrofission fragment angular distributions as a function of the electron incident energy, from this

work. The dashed curves are only to guide eyes. The single arrows indicate in the energy scale the mean values of fission channels thresholds taken from literature[4,7,13], and double arrows from the conclusions of this work.

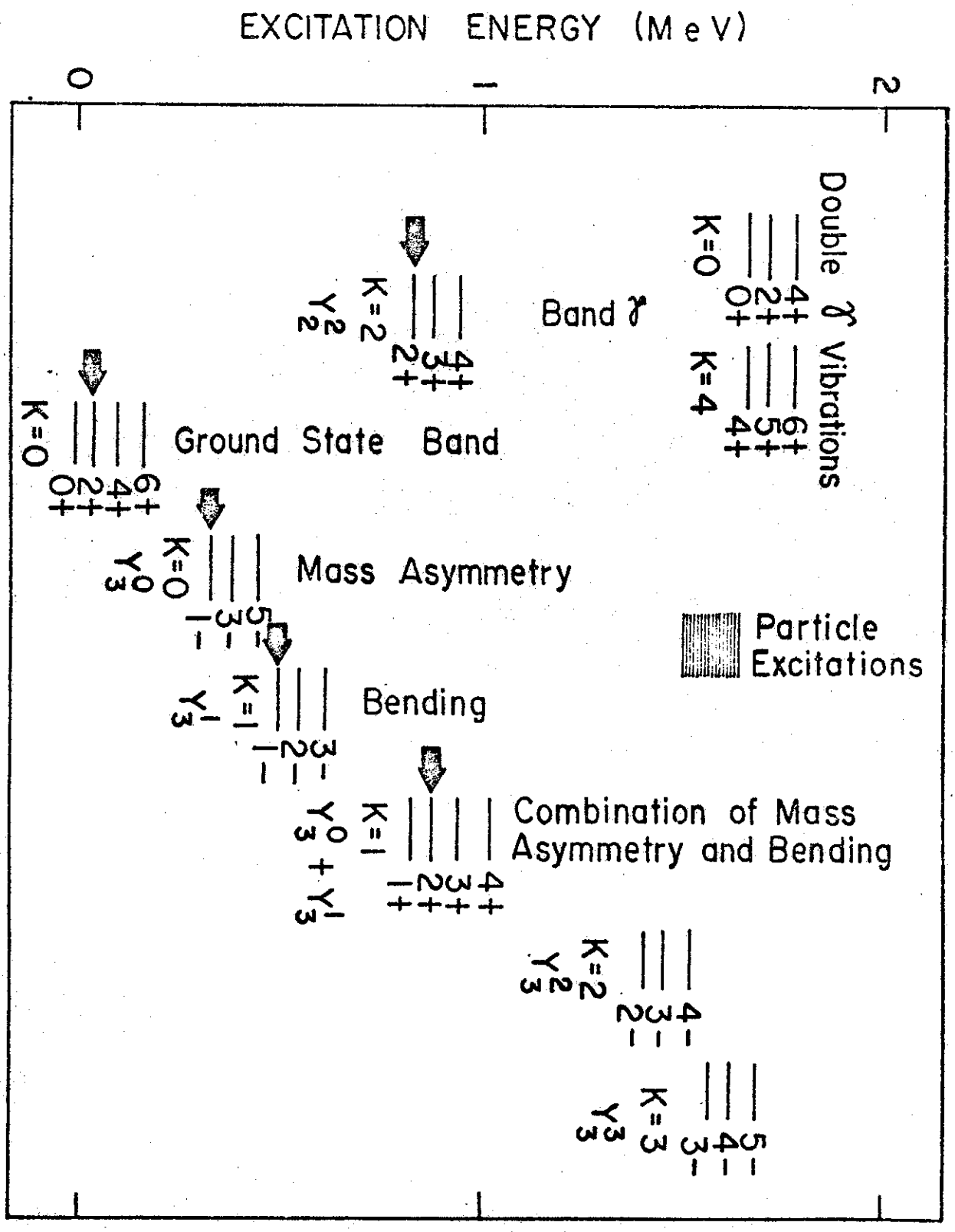
EXCITATION ENERGY (MeV)
0
1
2
Double γ Vibrations
K=0
K=4
Band γ
K=2
Ground State Band
K=0
Mass Asymmetry
K=0
Bending
K=1
Combination of Mass Asymmetry and Bending
K=1
K=2
K=3
Particle Excitations

Fig. 1

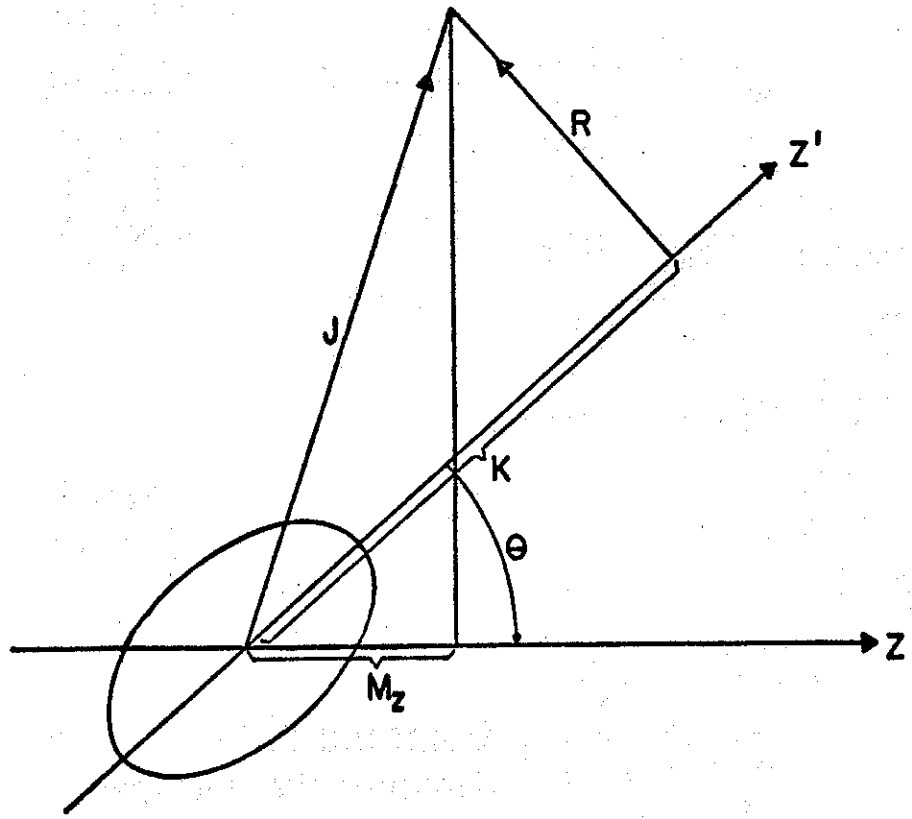

FIG.2

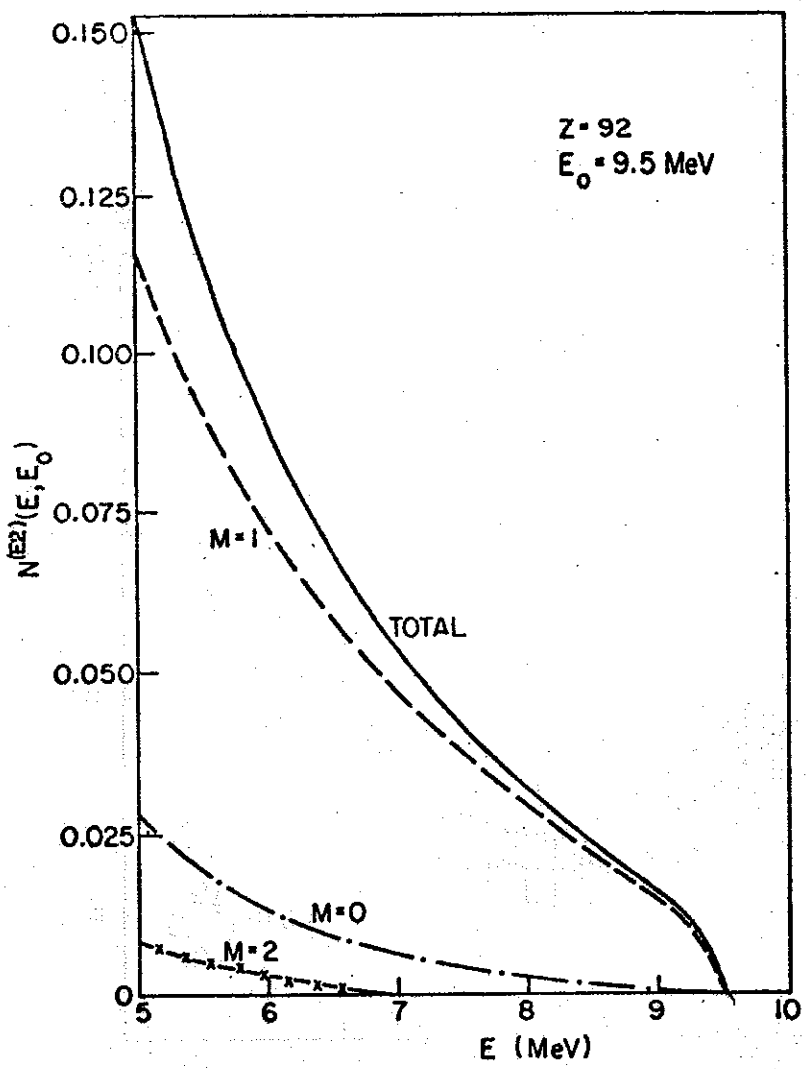
Z = 92
E_0 = 9.5 MeV
TOTAL
M=1
M=0
M=2
$N^{(E2)}(E,E_0)$
E (MeV)
0.150
0.125
0.100
0.075
0.050
0.025
0
5
6
7
8
9
10

Fig. 3b

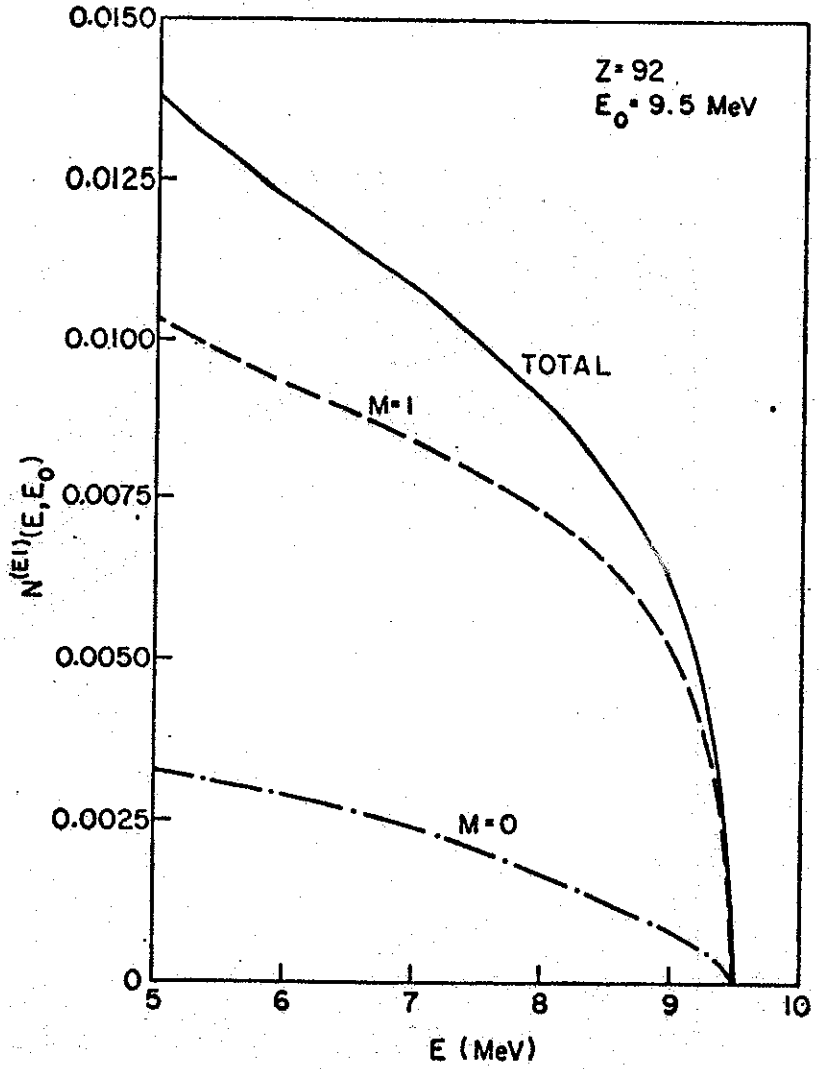
Z = 92
E_0 = 9.5 MeV
TOTAL
M=1
M=0
$N^{(E1)}(E,E_0)$
E (MeV)
0.0150
0.0125
0.0100
0.0075
0.0050
0.0025
0
5
6
7
8
9
10

Fig. 3a

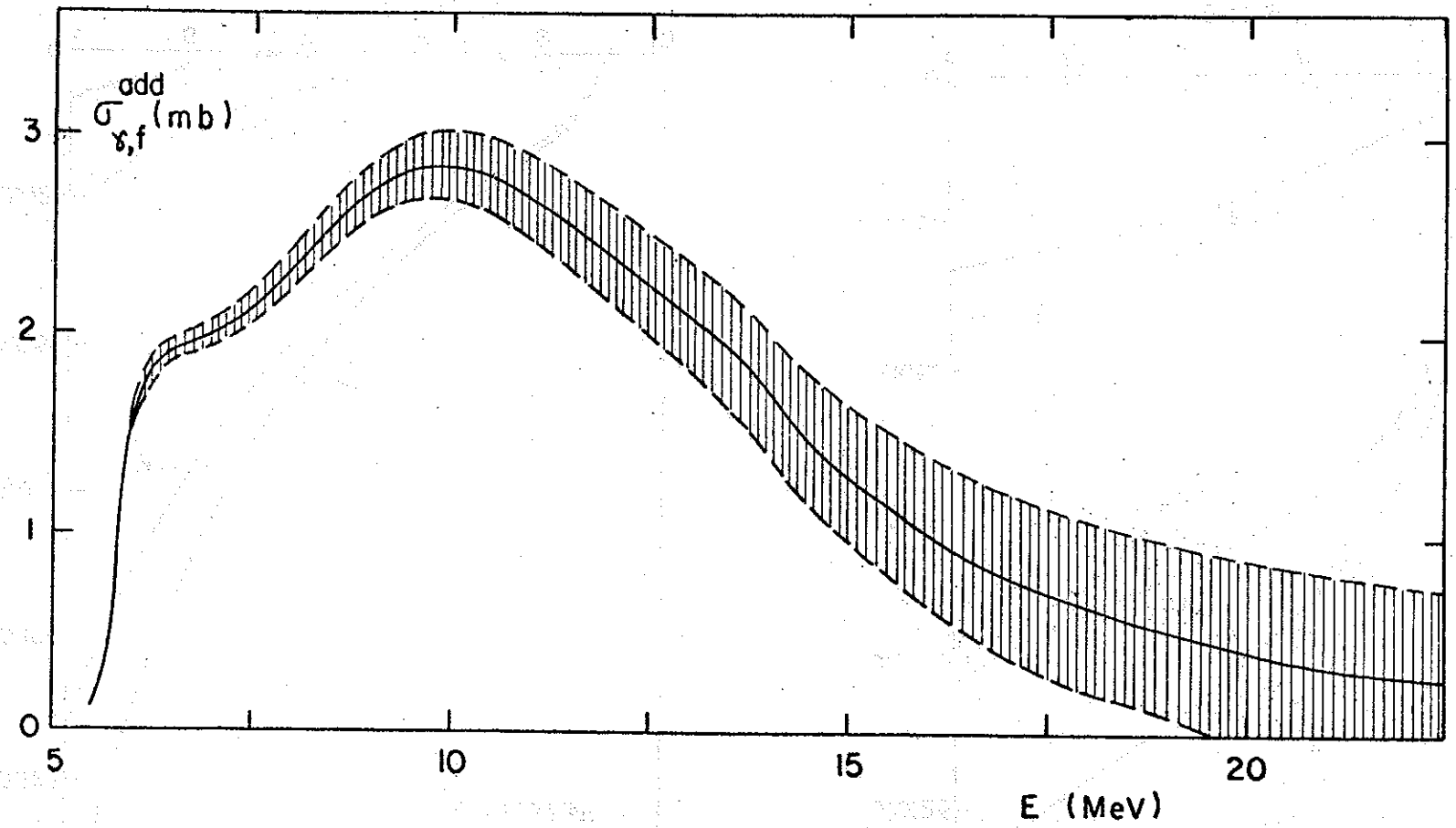

FIG. 4

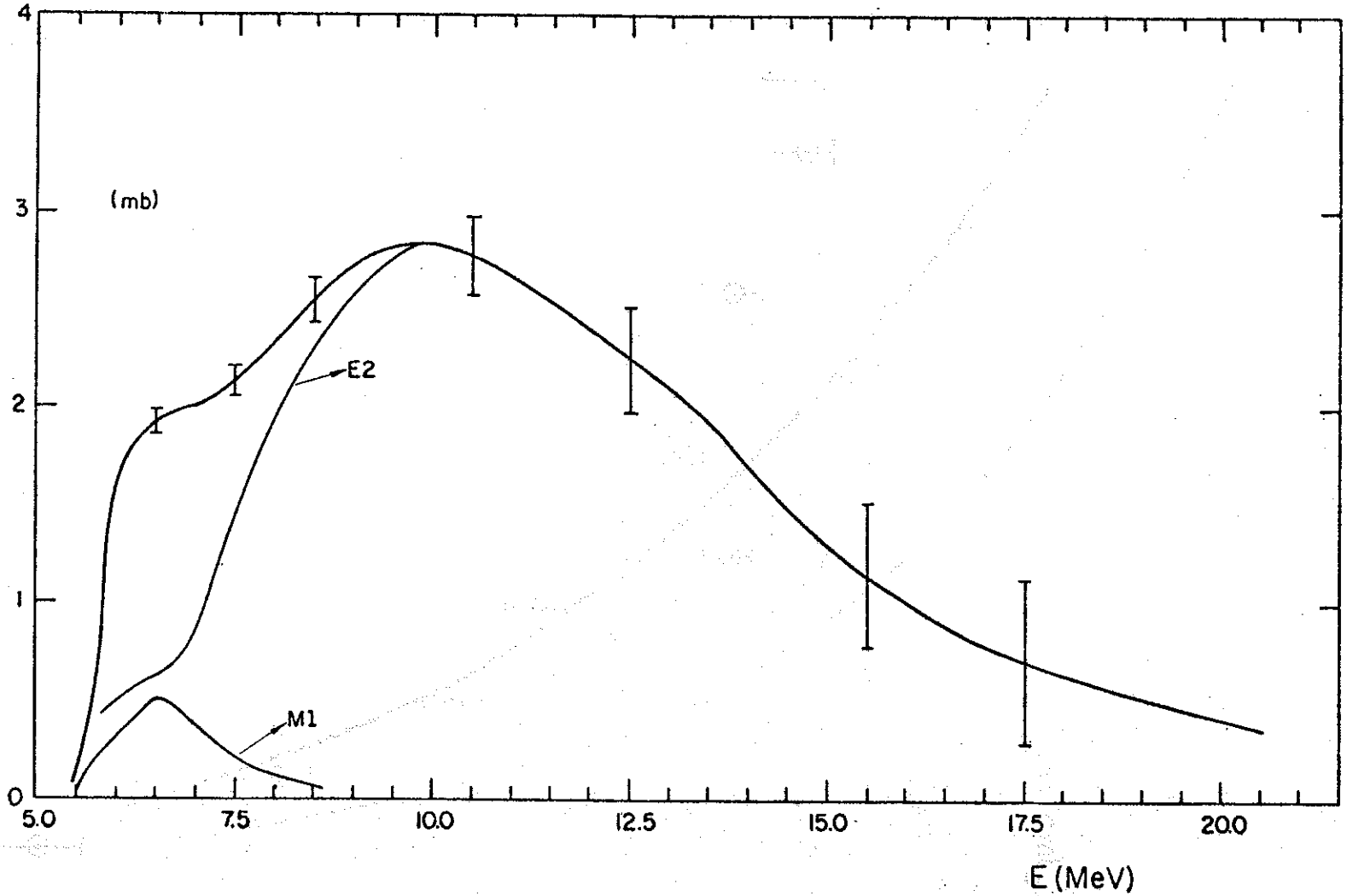

Fig. 5

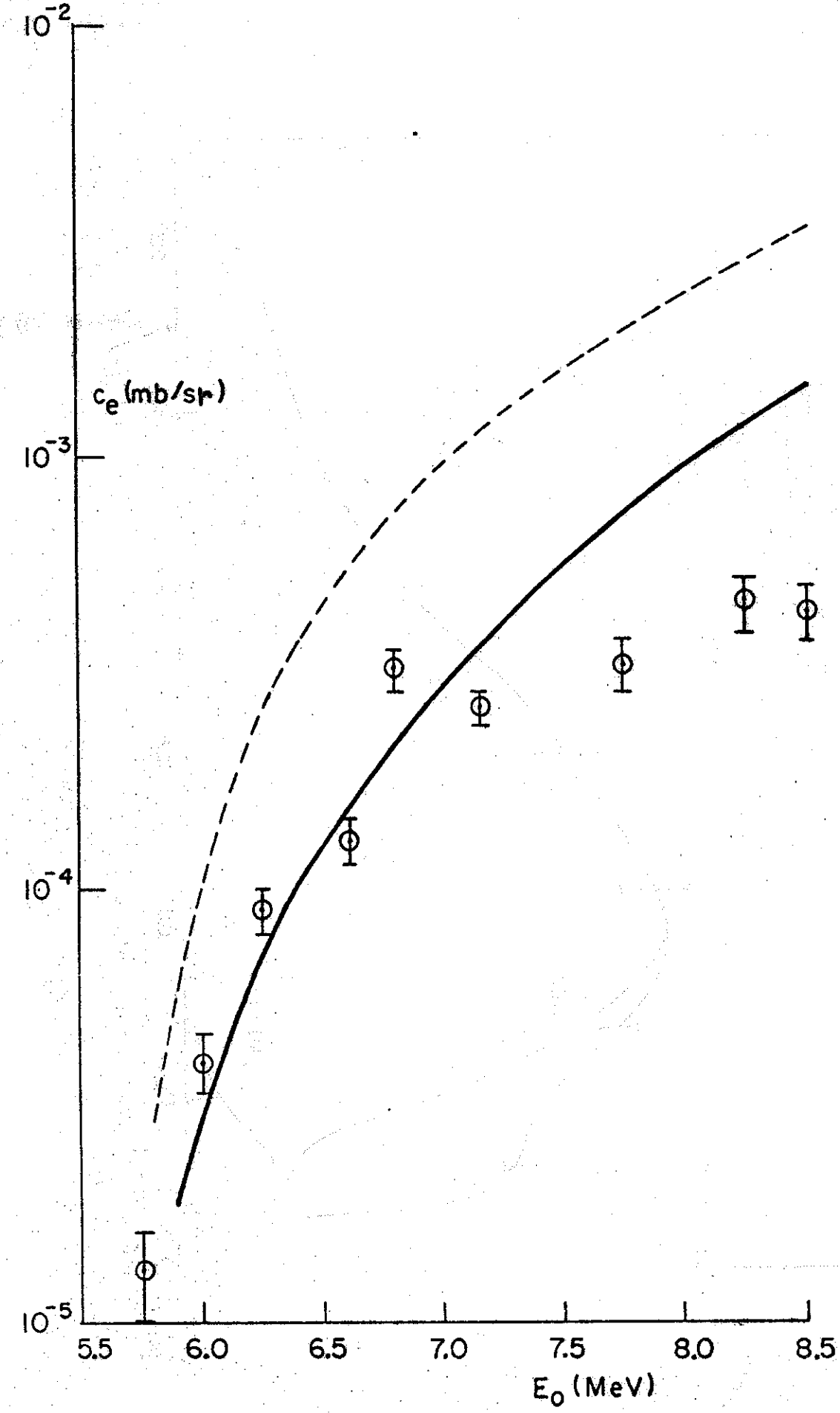

FIG. 6

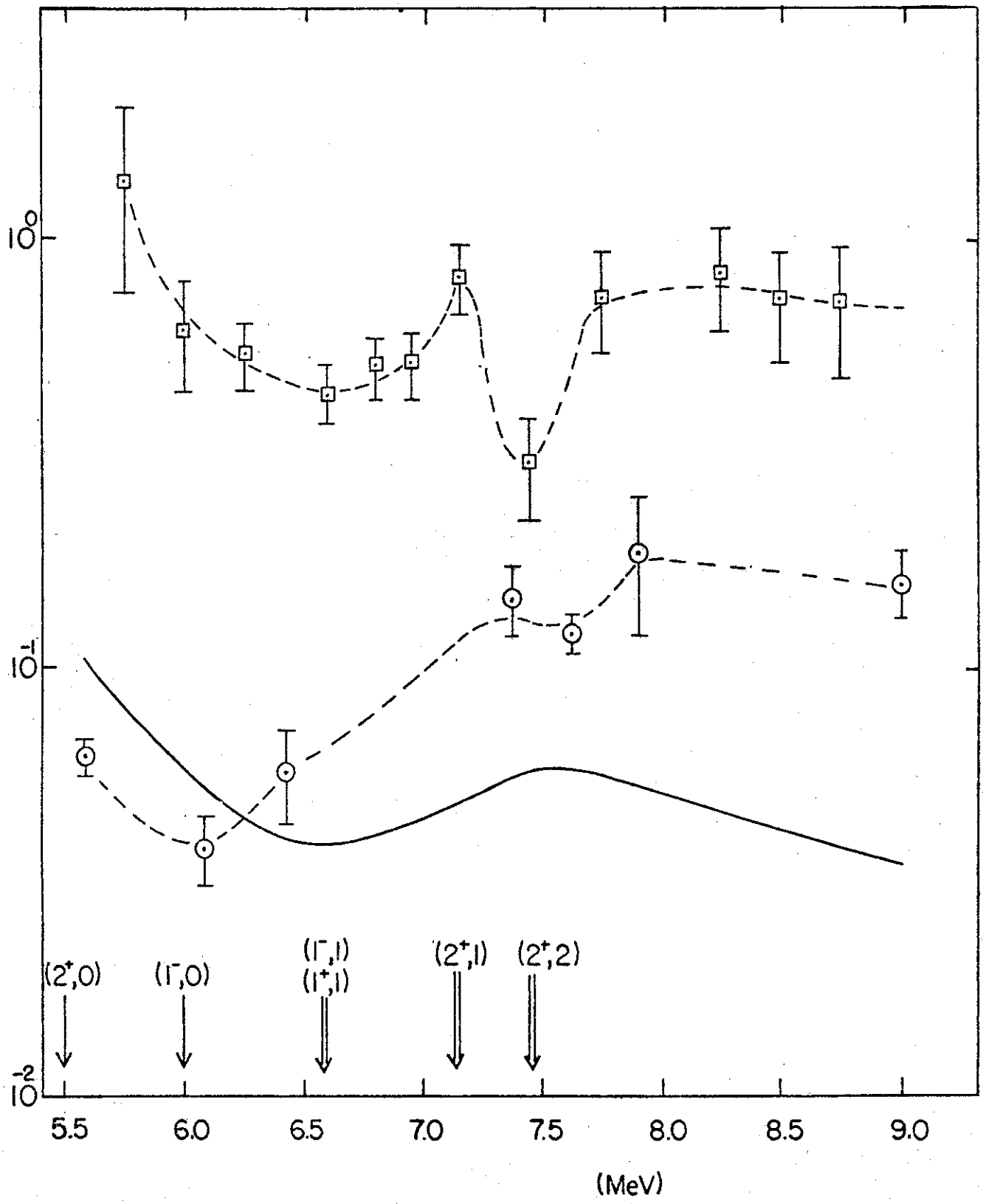

FIG. 7